

Article

Design and Optimization of the Inlet Header Structure in Microchannel Heat Exchanger Based on Flow Distribution Uniformity

Kaidi Zhang ¹, Wei Wei ^{1,2} , Yuwei Sun ^{2,3,4} , Qiang Wu ¹ , Min Tang ^{2,4} and Mingjian Lu ^{2,4,*}

¹ School of Transportation and Logistics Engineering, Wuhan University of Technology, Wuhan 430063, China; zkd@whut.edu.cn (K.Z.); wei_wei@whut.edu.cn (W.W.); 15872392061@163.com (Q.W.)

² National Engineering Research Center for Water Transport Safety (WTS Center, MoST), Wuhan University of Technology, Wuhan 430063, China; ywsun@whut.edu.cn

³ School of Naval Architecture, Ocean and Energy Power Engineering, Wuhan University of Technology, Wuhan 430063, China; tangmin@whut.edu.cn

⁴ Key Laboratory of Marine Power Engineering & Technology (MoT), Wuhan University of Technology, Wuhan 430063, China

* Correspondence: mingjian_lu@whut.edu.cn; Tel.: +86-27-8658-1992

Abstract: The flow distribution in a printed circuit heat exchanger (PCHE) is of great theoretical and practical significance in the Brayton cycle power generation system. For the straight barrel inlet header PCHE, when S-CO₂ flows in the PCHE, the structural types and working parameters of the inlet header and diversion zone may lead to differences in the flow distribution in each channel of the PCHE. This flow distribution difference affects the thermal hydraulic characteristics of the PCHE. A numerical simulation method was applied to explore the flow uniformity of the PCHE and the overall performance and analyze the influence of the type of straight barrel inlet header PCHE. Within each layer, the flow showed an uneven flow distribution, and the optimized inlet header was the tapered type. The results showed that when the taper angle varies from 6° to 9°, the flow distribution in each layer is relatively uniform. The comprehensive heat transfer performance of the straight-channel PCHE can be improved by 17.3–19.7%. Finally, the response surface and a genetic algorithm were combined to optimize the inlet header. The heat transfer performance of the optimized PCHE was improved by 19.7%.

Keywords: supercritical carbon dioxide (S-CO₂); printed circuit heat exchanger (PCHE); flow distribution; numerical simulation; thermal efficiency



Citation: Zhang, K.; Wei, W.; Sun, Y.; Wu, Q.; Tang, M.; Lu, M. Design and Optimization of the Inlet Header Structure in Microchannel Heat Exchanger Based on Flow Distribution Uniformity. *Appl. Sci.* **2022**, *12*, 6604. <https://doi.org/10.3390/app12136604>

Academic Editors: Fabio Polonara, Vítor António Ferreira da Costa, Sandro Nizetic and Alice Mugnini

Received: 9 June 2022

Accepted: 28 June 2022

Published: 29 June 2022

Publisher's Note: MDPI stays neutral with regard to jurisdictional claims in published maps and institutional affiliations.



Copyright: © 2022 by the authors. Licensee MDPI, Basel, Switzerland. This article is an open access article distributed under the terms and conditions of the Creative Commons Attribution (CC BY) license (<https://creativecommons.org/licenses/by/4.0/>).

1. Introduction

At present, the supercritical carbon dioxide (S-CO₂) Brayton cycle system, instead of the traditional steam Rankine cycle system, shows great potential in improving the photoelectric conversion efficiency of the system and reducing the power generation cost. S-CO₂ Brayton cycle power generation technology, with its significant technological and performance advantages, has considerable application potential in the utilization of ship flue gas waste heat, which is a critical way to improve the green level of ships and realize energy conservation and emission reduction in the shipping industry [1–3]. As one of the core components of the system, the S-CO₂ heat exchange precooler influences the system circulation efficiency. The printed circuit heat exchanger (PCHE) is considered the ideal S-CO₂ high-efficiency heat exchanger in the system due to its advantages of pressure reduction, large heat exchange area, good compactness, high heat exchange efficiency, and proper operation under high-intensity conditions [4].

The PCHE, which is a typical representative of a microchannel heat exchanger, contains hundreds of microchannels, and whether the flow in each microchannel is evenly distributed has a significant influence on the heat transfer characteristics of the PCHE. In

addition, considering that the physical properties of S-CO₂ (density, specific heat, viscosity, thermal conductivity, etc.) change with temperature, the flow state of S-CO₂ in the flow channel will also be affected [5,6]. Therefore, the study of flow allocation in microchannels of the PCHE is of great significance.

Most of the existing literature on PCHEs assumes that the flow distribution in the flow channels is uniform and that the operating condition is the steady state, ignoring the difference in the flow in the cross-section of the different flow channels and the influence of the inlet and outlet types on the flow distribution. An uneven flow distribution may lead to a decrease in the PCHE heat transfer performance. Pasquier [7] studied the influence of four different inlet header types on the flow non-uniformity of PCHEs. Koo [8] applied computational fluid dynamics (CFD) to optimize the mass flow rate distribution at the PCHE inlet, improving this distribution by 7.5%, eliminating the separation area near the surface, and reducing the pressure drop. Guo [9] studied the flow and temperature in homogeneities at the inlet end of the cross-flow heat exchanger. Multichannel plate heat exchangers are recommended for efficient power and propulsion systems. Chu [10] used a numerical simulation method to analyze the uneven distribution of large flow in the inlet header structure of high-temperature heat exchangers. Four kinds of improved intake headers were proposed, including an inclined baffle, a segmental baffle, a spiral baffle, and an improved spiral baffle. The results showed that all the proposed designs more or less improve the uniform flow distribution between the channels. Chu [11] analyzed four different inlet headers and proposed an improved header that significantly reduced flow inhomogeneity. Ma [12] established a new prediction model to predict the uneven flow distribution in PCHEs and found that an increase in the channel length could improve the uneven flow distribution. Fan [13] studied the local and global thermal hydraulic properties of different PCHEs using supercritical liquefied natural gas (LNG) and liquid nitrogen by numerical methods and found that flow separation and recirculation at corners inhibited heat transfer and increased the pressure drop. Smoothness of the corners facilitates heat transfer and leads to a reduction in hydraulic resistance. At constant mass flow, a sinusoidal channel can reduce the pressure drop by 8.3% and increase the heat transfer coefficient by 2.9% compared with a serrated channel with a sharp angle. Shi [14] studied the optimal structure of the inlet header using an alternative model combined with a genetic algorithm and reduced the flow inhomogeneity of the heat exchanger. However, these studies were primarily concerned with the thermal and hydraulic properties of individual heat exchanger units. Xu [15] proposed the optimal size of a fixed volume PCHE and simulated two boundary conditions of the PCHE. When the volume of the PCHE was fixed, the heat transfer rate and pressure drop were selected as optimization objectives to obtain the optimized structure. Lalot [16] studied the difference in PCHE heat transfer performance caused by uneven flow. The results showed that a small flow inhomogeneity can lead to a large loss in heat transfer efficiency. An inlet header type was further proposed to improve the flow uniformity and overall performance of the heat exchanger at the cost of a slight increase in the pressure drop. Zhang [17] studied different distributor configurations used in plate-fin heat exchangers. Some design features of the distributor can lead to serious uneven flow distribution. Experimental results showed that the optimized distributor is effective in improving the heat transfer performance of the heat exchanger. Yang [18] developed a mathematical model combined with numerical simulation to evaluate the influence of flow inhomogeneity in a multichannel heat exchanger. An improved quasi-S-shaped head structure was proposed, effectively reducing heat transfer deterioration due to non-uniformity problems. Ke [19] used a numerical model to study the flow field distribution and resistance characteristics of PCHE plates under different flow field distributions. The results showed that the abrupt change in fluid angle can be greatly reduced by using diffuser plates with equal internal and external radii. This can also weaken the fluid diversion at the channel entrance and reduce the flow distribution imbalance in the channels. Therefore, the flow uniformity can be improved, and the pressure drop between the PCHE inlet and outlet can be reduced. Tereda [20] proposed a relationship between

the orifice size and flow distribution by measuring the non-uniformity of flow from the port to the channel and the mass flow in the channel in the plate heat exchanger, which provides an important basis for reducing flow non-uniformity in plate heat exchanger design. Anbumeenaksh [21] experimentally studied three header types, rectangular, trapezoidal, and triangular, and two types of inlet configurations. The results showed that the vertical inlet configuration had less non-uniformity than the flat configuration at low flow rates. Redo's [22] study described the development of an improved vertical header with a two-compartment structure designed to improve the flow distribution. Double-compartment headers can increase the fluid flow distribution from approximately 30% to 80% at low inlet mass fluxes, and the liquid Reynolds numbers are typically higher than those with conventional headers. Zoljalali [23] examined the influence of each geometric factor by using a set of CFD models modeled in the finite element software COMSOL Multiphysics. The results showed that increasing the number of channels, spacing of channels, and concavity and decreasing the channel width positively affect the flow distribution between channels. The prediction model was obtained by training a neural network based on the CFD model. Niroomand [24] developed a new model to show how the asymmetrical flow distribution caused by heat affects the performance of heat exchangers and found that the optimal layer arrangement is helpful for eliminating the asymmetrical distribution caused by heat in heat exchangers. Kim [25] designed two arrangement modes in the horizontal and vertical directions for the experimental helium–water loop and found that a horizontal arrangement would lead to uneven distribution, thus resulting in differences from simulation results. Existing experimental studies focus on the thermal hydraulic characteristics of PCHEs and the construction of related heat transfer and pressure drop correlations. Limited by the small size and high pressure of PCHE channels, there are few experimental observation studies on the flow patterns in PCHE channels at present.

Based on the investigation and analysis of the literature, the research on S-CO₂ Brayton cycle power generation is still in the development stage. Studies on flow and heat transfer in PCHE belong to the field of applied research, and most of them focus on the establishment of the heat transfer correlation and the design of PCHEs [26–29]. Nevertheless, most studies are based on the assumption that the flow in the PCHE channel is evenly distributed, and few studies consider the uniformity of the flow distribution in each channel of the PCHE, PCHE pressure drops, and heat transfer efficiency, mainly because the flow channel is small. The internal flow parameters are difficult to measure. Thus, there are still problems in the study of PCHE heat transfer characteristics. For the straight barrel inlet header PCHE channel, the non-uniform flow distribution phenomenon is caused by the structure itself. If a guide plate is set up in the diversion area, then a higher flow can be obtained in the middle of the channel. Nevertheless, the additional guide plate structure is bound to cause a diversion area with increased pressure drop, leading to deterioration of the PCHE hydraulic characteristics on the whole, thus affecting the turbine inlet pressure in the Brayton cycle, which is a pyrrhic gain. In addition, due to the high operating pressure of the system, the setting of the guide plate may cause local stress concentration, which is not conducive to safe and stable operation of the system. Therefore, the design of the existing straight barrel inlet header PCHE must be optimized to improve the non-uniformity of the flow distribution in each layer of the PCHE so that the flow in the straight barrel inlet header PCHE can be generally evenly distributed.

This paper is aimed at the optimization structure of straight barrel inlet header PCHE. When S-CO₂ flows in the PCHE, the structural types and working parameters of the inlet header and diversion zone may lead to differences in the flow distribution in each channel of the PCHE, and the uniformity of the flow distribution increases with increasing PCHE scale. This difference in flow distribution affects the thermal hydraulic characteristics of the PCHE and further reduces the comprehensive performance of the Brayton cycle power generation system. Therefore, a numerical simulation method is proposed to explore the influence of flow uniformity on the overall performance of the PCHE and improve the

structure of the straight barrel inlet header PCHE to optimize the S-CO₂ distribution in the PCHE flow channel.

2. Flow Distribution Characteristics of the Straight Barrel Inlet Header PCHE

The PCHE used in the studied test platform contains a total of 20 layers of heat exchange plates (10 layers for cold plates and 10 layers for hot plates). The structure of the PCHE is shown in Figure 1. The inner diameter of the inlet and outlet headers is 10 mm, the distance from the center of the inlet and outlet headers to the microchannel area is 32.91 mm, the cross-section of the microchannel is a semicircle with a diameter of 2 mm, and each layer of the heat exchange plate contains 10 straight channels with spacing of 1 mm. The length of the microchannel is 295.20 mm; that is, the number of microchannels on the hot and cold sides is 100. The heat transfer between hot and cold fluids occurs as a counter flow.

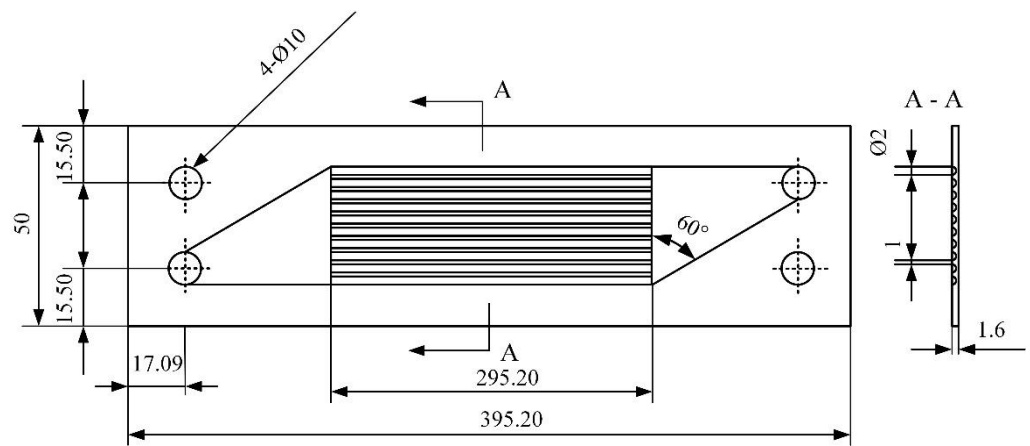


Figure 1. Structure of the PCHE.

2.1. Physical and Numerical Models

To explore the influence of the flow distribution law in the PCHE on the thermal hydraulic characteristics, the basic structure of the straight barrel inlet header PCHE must be analyzed. The single-side flow channel model of the straight-channel PCHE is shown in Figure 2, which includes five parts: inlet header, inlet diversion area, microchannel area, outlet confluence area, and outlet header. Given the complexity of the straight-channel PCHE structure, the simplified assumptions in this section are as follows:

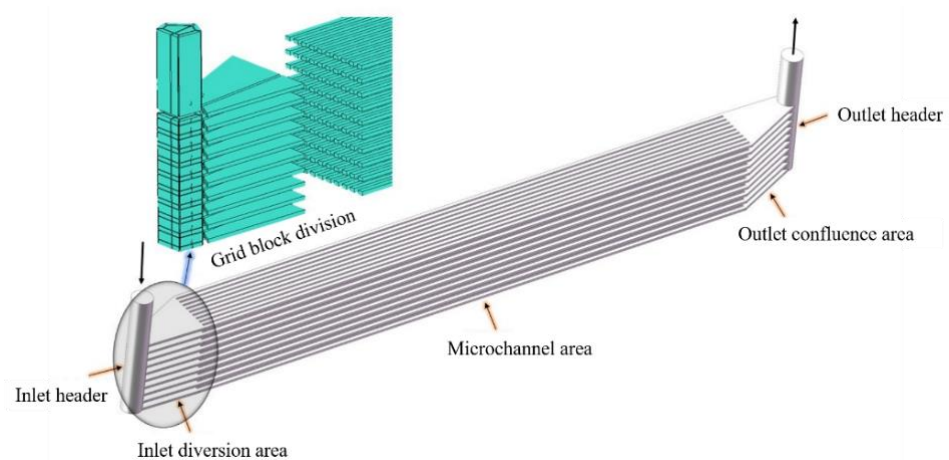


Figure 2. Single-side flow channel model and grid block division strategy of the straight-channel PCHE.

(1) The junction between the semicircular microchannel area and the inlet diversion area is tangent at the bottom of the heat exchanger plate, and the quality of the mesh division in the diversion area is deficient. Therefore, the semicircular flow channel is simplified into a rectangular flow channel according to the hydraulic diameter, which is convenient for improving the mesh quality.

(2) Ref. [30] shows that the primary thermal resistance in S-CO₂–water heat transfer is on the S-CO₂ side, so only the S-CO₂ side flow channel needs to be calculated, and a constant wall temperature is given on the S-CO₂ side.

The grid block partitioning strategy is shown in Figure 2, where the inlet and outlet headers are divided into O-grids to improve the grid quality. To ensure the accuracy of numerical simulation calculations, the fluid domain is divided by hexahedral grids. The thickness of the first layer grid at the interface is 0.01 mm, the growth rate is 1.2, and the final orthogonal value is above 0.55. Grid independence was verified and the number of grids finally was determined, about 12 million. In the single-side flow channel model of the straight-channel PCHE, the inlet boundary is a mass flow rate, and the outlet boundary sets a specific pressure. The upper and lower parts of each heat exchanger plate are closest to the fluid on the other side, and the temperature is set as constant. The other wall surfaces are simplified as adiabatic walls. The NIST real gas model in Fluent is used to simulate the flow properties of S-CO₂ in the PCHE. This model can consider the influence of temperature and pressure changes on the physical properties of S-CO₂. The *SST k- ω* model is used for the turbulence model. SIMPLE is used for the discrete algorithm. The second-order discrete scheme is used for the pressure, the second-order upwind method is used for the momentum and density, and the second-order upwind scheme is used for the turbulent kinetic energy and turbulent dissipation rate. The convergence criterion is 10^{-3} .

To verify that the numerical model in this section can be used to simulate the flow distribution uniformity in the PCHE, as a validation, the experimental data in Ref. [10] were selected to validate our model. Figure 3 shows that the Nusselt number of the simulation results and experimental data are essentially consistent. The average error is within 10%, and the maximum error is 12.5%. This shows that the numerical model can simulate the flow distribution uniformity in the PCHE.

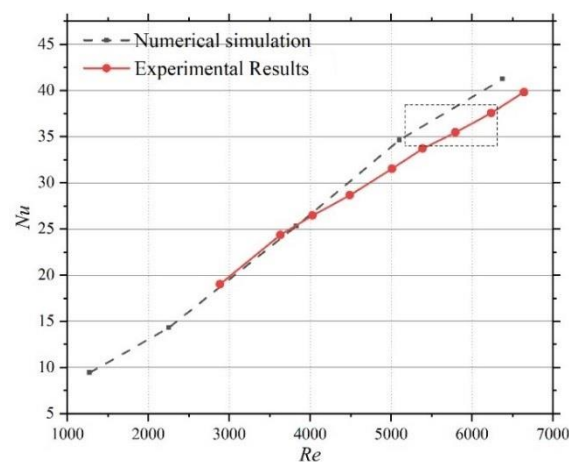


Figure 3. Numerical model validation (Experimental Results [10]).

To explore the influence of the straight barrel inlet header PCHE on the flow rate, the working conditions listed in Table 1 are set for numerical simulation.

Table 1. Simulation working conditions.

Number	Pressure/MPa	Flow Rate/(kg·s ⁻¹)	Inlet Temperature/K	Wall Temperature/K	Re
1		0.01			1275.8
2		0.02			2551.6
3	9.5	0.03	305	333	3827.4
4		0.04			5103.2
5		0.05			6379.0

The flow non-uniformity in the PCHE can be divided into three kinds according to different objects of attention: the non-uniformity in each layer, the non-uniformity in each flow channel, and the overall non-uniformity, which can be used to characterize the degree of flow distribution deviation from the uniform flow distribution in the PCHE. The PCHE is assumed to have i layers of heat exchanger plates ($i = 1, 2, \dots, n$), each layer has j flow channels ($j = 1, 2, \dots, n$), and the flow rate in flow channel j of layer i is denoted as c_{ij} . Then, the average flow rate of the flow channels is

$$c_{ave} = \frac{\sum_{i=1}^N \sum_{j=1}^n c_{ij}}{Nn} \tag{1}$$

where c_{ave} is the average flow rate of the flow channels, kg/s.

The average flow rate of the layers is

$$p_{ave} = \frac{\sum_{i=1}^N \sum_{j=1}^n c_{ij}}{N} \tag{2}$$

The channel non-uniformity of each flow channel is defined as

$$CN_{ij} = \frac{|c_{ij} - c_{ave}|}{c_{ave}} \tag{3}$$

where CN_{ij} is the non-uniformity of each flow channel. The plate non-uniformity of each layer is defined as

$$PN_i = \frac{\left| \sum_{j=1}^n c_{if} - p_{ave} \right|}{p_{ave}} \tag{4}$$

where PN_i is the non-uniformity of layer i . The overall non-uniformity of the straight barrel inlet header PCHE is defined as

$$ON = \sum_{i=1}^N \sum_{j=1}^n CN \tag{5}$$

where ON is the overall non-uniformity.

The values of the above non-uniformities differ in size. For the convenience of understanding and analysis, the standard deviations of the various non-uniformities are adopted to normalize them. The standard deviation of the overall non-uniformity is

$$\sigma_o = \sqrt{\sum_{i=1}^N \sum_{j=1}^n (CN_{ij} - ON/Nn)^2 / nN} \tag{6}$$

where σ_o is the standard deviation of the overall non-uniformity. The standard deviation of the non-uniformity of each layer is

$$\sigma_p = \sqrt{\sum_{i=1}^N \left(PN_i - \sum_{i=1}^N PN/N \right)^2 / N} \tag{7}$$

where σ_p is the standard deviation of the non-uniformity of each layer. The standard deviation of the non-uniformity of each flow channel of the layer i heat exchanger plate is

$$\sigma_{i,c} = \sqrt{\sum_{j=1}^n \left(CN_{tj} - \sum_{j=1}^n CN_{tj}/n \right)^2 / n^2} \tag{8}$$

where $\sigma_{i,c}$ is the standard deviation of the non-uniformity of each flow channel of the layer i heat exchanger plate.

2.2. Flow Distribution Characteristics of the Straight Barrel Inlet Header PCHE

The internal flow characteristic is analyzed under the conditions of pressure 9.5 MPa, flow rate 0.05 kg/s, inlet temperature 305 K, and wall temperature 333 K. Figure 4 shows the numbering rules for the layers and flow channels.

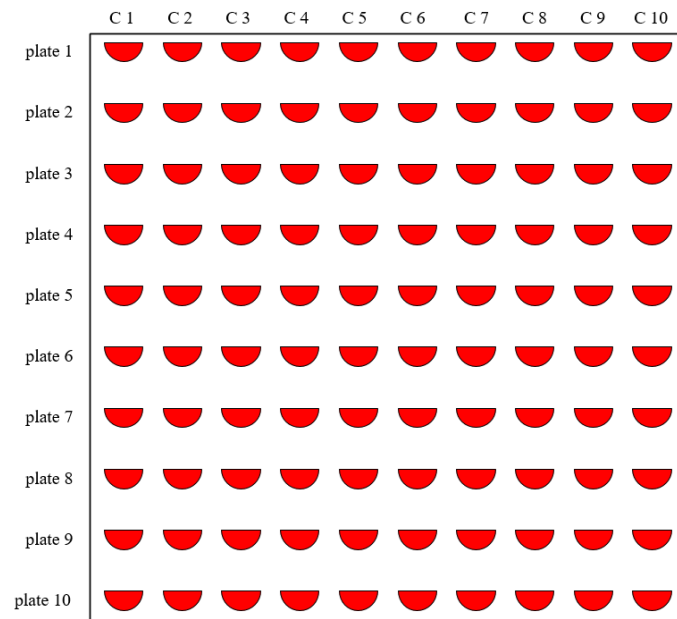


Figure 4. Schematic diagram of the PCHE inner layer number and flow channel number.

Figure 5 shows the flow distribution at each channel. Based on an analysis of the flow characteristic, inside the straight-channel PCHE, a significant difference between the flow distributions in each layer can be found. The flow distribution within the flow channel in a particular layer exhibits relatively small differences. The single current flow gradually increases with increasing layer number, and the flow distribution on both sides is higher than that in the middle. In the whole straight barrel inlet header PCHE, the flows in channels C1 and C10 of the plate10 heat exchanger plate are the maximum. In contrast, the flow in channel C6 of the plate1 heat exchanger plate is the minimum, and the flow in channel C1 of the plate5 heat exchanger plate is closest to the uniform flow distribution state.

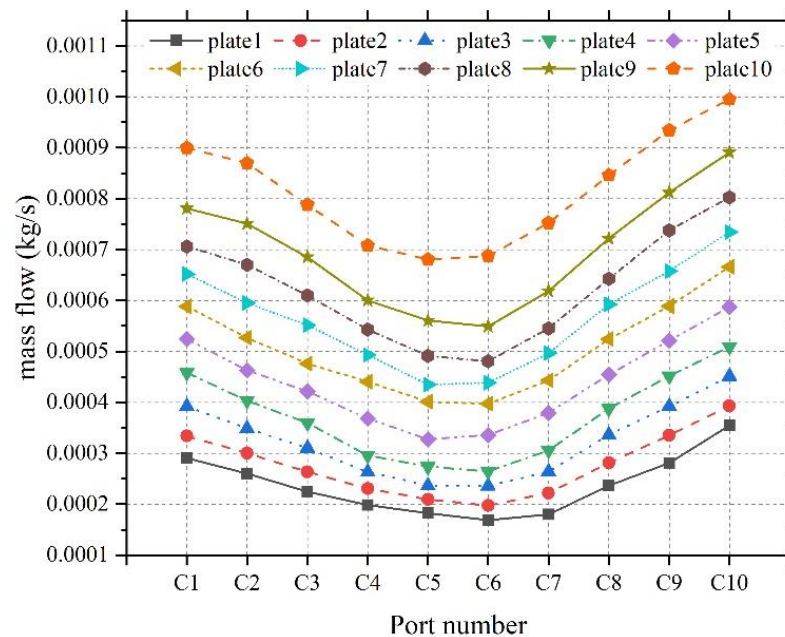


Figure 5. Statistical diagram of the flow distribution in each channel.

Because the direction of the inlet header is perpendicular to the direction of the heat exchanger plates, the flow is similar to that of a confined impact jet. When a flow impacts a disk, the velocity is evenly distributed in 360°. When the disk shape is gradually reduced from 360° to 180°, 90°, and 60° by a wall, the existence of the wall prevents the flow on the disk from expanding in all directions, resulting in the velocity in the region near the border of the disk being much higher than that in the region away from the wall. The flow velocity distribution in the diversion area of the straight barrel inlet header PCHE is similar to that in the case with an angle of 60°. Therefore, Figure 5 shows that the flow distribution on both sides of the straight barrel inlet header PCHE is higher than that in the central flow channel.

Figure 6 shows the flow proportion curves of each heat exchanger plate layer under different inlet flow rate conditions. A higher inlet flow rate has almost no influence on the flow proportion of each layer. On the one hand, as the structure of the inlet header and heat exchanger plate is similar to that of an impact jet, according to the Bernoulli theory, the velocity energy is converted into pressure energy at the bottom of the inlet header. With increasing PCHE layer number, the pressure is greater at the entrance of the heat exchanger plate, and the more flow is distributed. On the other hand, each heat exchanger plate layer, in turn, leads to a gradual reduction in the average speed of the flow along the header, slowly resulting in a higher static pressure. In contrast, the velocity in the central part of the header is higher. As a result of the no-slip wall boundary conditions of each heat exchanger plate layer, near the entrance, the velocity is low, and the low-speed flow in the peripheral region of the header cannot protect against pressure gradient flow [31]. Therefore, flow separation leads to the formation of a backflow zone at the bottom of the header. Hence, the proportion of flow distribution in each layer increases with the PCHE layer number. Further statistics show that the standard deviation of the overall non-uniformity is 0.226. The standard deviation of the non-uniformity of each layer (σ_p) is 0.188 under the condition that the flow rate is 0.05 kg/s. The standard deviation of the non-uniformity of each flow channel of each heat exchanger plate layer ($\sigma_{i,c}$) is shown in Table 2. $\sigma_{i,c}$ and σ_p are equivalent in order of magnitude. The flow distribution in the straight barrel inlet header PCHE is uneven between each heat exchanger plate layer and between the flow channels of a single-layer heat exchanger plate.

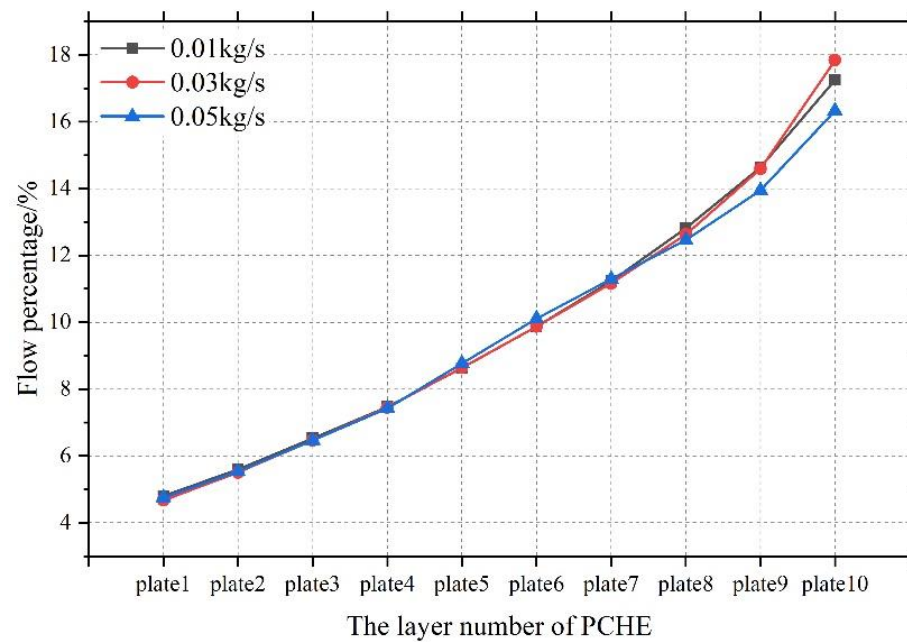


Figure 6. Flow distribution ratio of each layer.

Table 2. Statistics of the standard deviation of the non-uniformity of each flow channel of each heat exchanger plate layer.

<i>i</i>	C 1	C 2	C 3	C 4	C 5	C 6	C 7	C 8	C 9	C 10
$\sigma_{i,c}$	0.116	0.125	0.144	0.152	0.099	0.096	0.153	0.209	0.23	0.214

In a single flow channel, the non-uniform flow distribution phenomenon in the heat exchanger plate layers is caused by the structure itself. If a guide plate is set up in the diversion area, then a higher flow can be obtained in the middle of the channel. Nevertheless, the additional guide plate structure is bound to cause a diversion area with increased pressure drop, leading to the deterioration of the PCHE hydraulic characteristics on the whole, thus affecting the turbine inlet pressure in the Brayton cycle, which is a pyrrhic gain. In addition, due to the high operating pressure of the system, the setting of the guide plate may cause local stress concentration, which is not conducive to safe and stable operation of the system. Therefore, the design of the existing straight barrel inlet header PCHE must be optimized to improve the non-uniformity of the flow distribution in each layer of the PCHE so that the flow in the straight barrel inlet header PCHE can be rather evenly distributed and the system can run under conditions close to the design point.

3. Flow Distribution Characteristics of the Tapered Header

Under the condition of countercurrent heat transfer, there are two arrangement modes, as shown in Figure 7. In the actual PCHE cold and hot side header arrangement, when the inlet headers of the cold and hot sides are on different sides and the outlet headers are also on different sides, this is simply referred to as “different side in and different side out”; when the cold and hot side inlet headers are on the same side and the outlet headers are also on the same side, this is termed “same side in and same side out”.

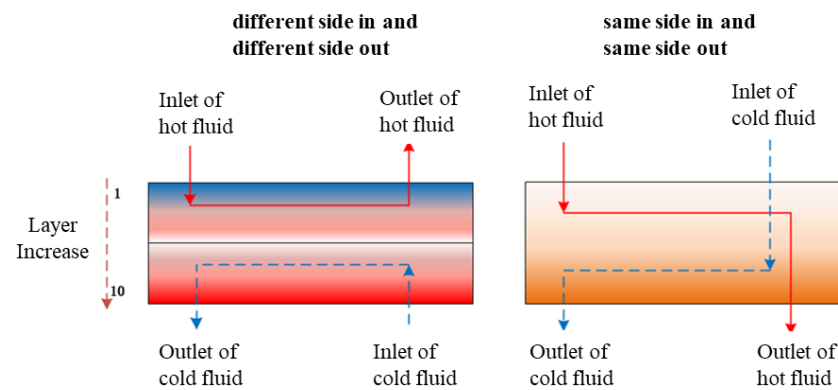


Figure 7. PCHE cold and hot side inlet and outlet header layout.

In this section, based on the simulation results, the flow distribution in the heat exchanger plate layer away from the entrance of the PCHE inlet header is found to be the highest, and that in the heat exchanger plate layer near the entrance of the PCHE inlet header is found to be the lowest. Under the different inlet and outlet configuration, the hot fluid has the highest flow distribution in the 10th heat exchanger plate layer, while in the first layer, the hot fluid has a minor flow distribution. The flow distribution of the cold fluid is the highest in the first heat exchanger plate layer. The flow distribution is the lowest in the 10th heat exchanger plate layer. For the same inlet and outlet configuration, the flow distribution of hot and cold fluids is the highest in the 10th heat exchanger plate layer, and the flow distribution is the lowest in the first heat exchanger plate layer.

For the “different side in and different side out” arrangement, the PCHE heat transfer unit in the first layer has less hot fluid flow and more cold fluid flow, which leads to a mismatch of the cold and hot side flows in the same heat transfer unit and excess cooling capacity of the cold fluid. However, in the PCHE heat transfer unit in the 10th layer, there is more hot fluid flow and less cold fluid flow, which leads to insufficient cooling capacity of the cold fluid, similar to the situation of dry burning in a boiler with less flow distribution for the high heat load. (Note: Heat transfer unit here refers to a cold-side heat exchanger plate layer and a hot-side heat exchanger layer plate constituting a cold and heat transfer unit layer.)

For the “same side in and same side out” arrangement, the flow distributions of both cold and hot fluids are small in the PCHE heat transfer unit in the first layer, while the flow distributions of both cold and hot fluids are enormous in the PCHE heat transfer unit in the 10th layer. Matching of cold and hot flows is adequately realized, and matching of the flows corresponds to matching of the heat loads, which can give full play to the cooling capacity of the cold fluid.

For the “same side in and same side out” arrangement, the flow rates and heat loads on the hot and cold sides match, but there is a significant asymmetry in the flow distribution from the first layer to the tenth layer. In the “different side in and different side out” arrangement, the flow rates and heat loads on the hot and cold sides are very different. Therefore, the uneven distribution of the flow rate must be improved to improve the comprehensive heat transfer performance of the PCHE.

According to the analysis results, the lower the layer number is, the more flow rate is distributed by the heat exchanger plate. Therefore, optimizing the configuration of the header into a tapered type can be considered so that when S-CO₂ flows downward in the tapered area, the pressure energy and velocity energy at the entrance of the heat exchanger plate in each layer from top to bottom remain unchanged. The backflow dead zone at the bottom of the header is eliminated to realize uniform distribution of the flow of the heat exchanger plate in each layer. Figure 8 shows the structure diagram of the tapered header. The magnitude of different taper angles θ represents the rate at which pressure energy is converted into velocity energy along the flow direction of the tapered area. Limited by the structural characteristics of the model, the diameter of the top circle is constant at

$d_1 = 10$ mm, and the distance between the first heat exchanger plate and the tenth heat exchanger plate is 29.8 mm. Assuming that the bottom circle diameter d_2 is 0, the maximum value of the angle θ is 18.55° ; that is, angle θ ranges from 0° to 18.55° . In this paper, 3° to 15° models which inlet mass flow is 0.05 kg/s are selected for numerical simulation to explore the influence of different structural parameters on the non-uniformity of the flow distribution in each layer. The d_2 corresponding to specific angles is listed in the following Table 3.

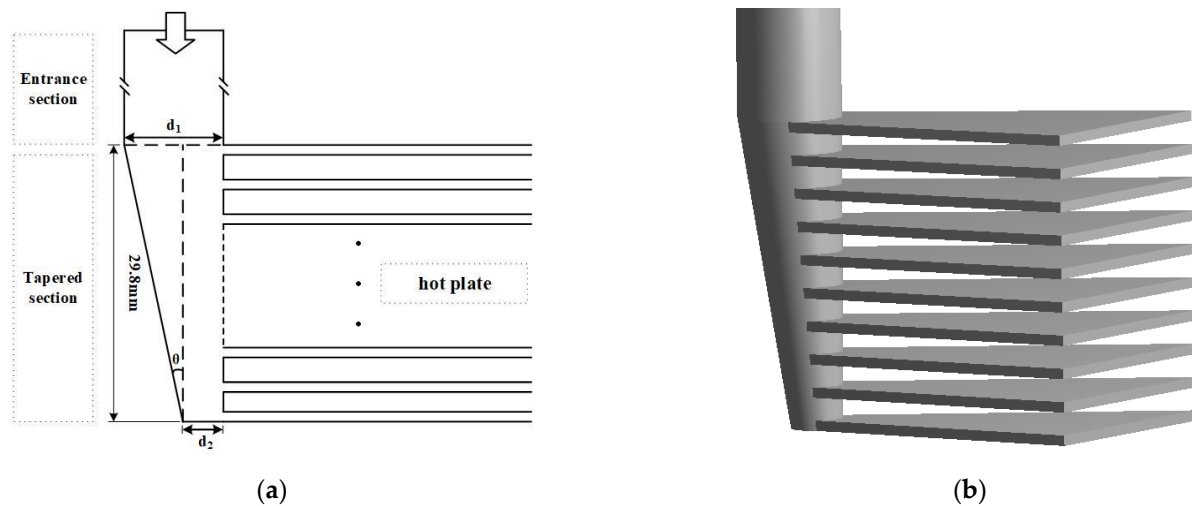


Figure 8. Structure diagram of a tapered header. (a) Schematic diagram, (b) local structure.

Table 3. Structural parameters of the tapered header.

Taper Angle $\theta/^\circ$	3	6	9	12	15
d_2/mm	8.4	7.0	5.0	3.6	2.0

Figure 9 shows the proportion of the flow distribution in each layer of the models with different taper angles. The taper angle of the inlet header has a significant influence on the proportion of the flow distribution in each layer of the straight barrel inlet header PCHE. As mentioned above, $\theta = 0^\circ$ corresponds to the original configuration. The flow ratio gradually increases with the layer number. The deviation between the maximum and minimum values reaches 243%, significantly deviating from the state of uniform flow distribution in all layers. With the taper angle gradually increasing from 0, the flow distribution in each layer can be found to fundamentally follow a monotonic change law. In layer 1, the flow distribution of the heat exchanger plate gradually increases. In the 10th heat exchanger plate layer, the flow distribution decreases, and in layers 5 and 6, the flow distribution of the heat exchanger plate remains around 10%, the closest to a uniform flow distribution state. This occurs because as the taper angle θ gradually increases, the diameter d_2 of the bottom circle of the header slowly decreases, and the inclination degree of the tapered header slowly increases, leading to a more significant proportion of pressure energy being converted to velocity energy along the flow direction of the header. The larger the velocity energy is, the less flow is distributed to the layer. Therefore, as the taper angle θ increases, the average slope of the flow distribution ratio curve of each layer of the straight barrel inlet header PCHE gradually decreases from positive to 0 and then negative. On the whole, when $\theta = 6^\circ$ and $\theta = 9^\circ$, the flow distribution in each layer is approximately 10%. Uniform flow distribution in each layer of the PCHE can be considered to be realized under these structural parameters.

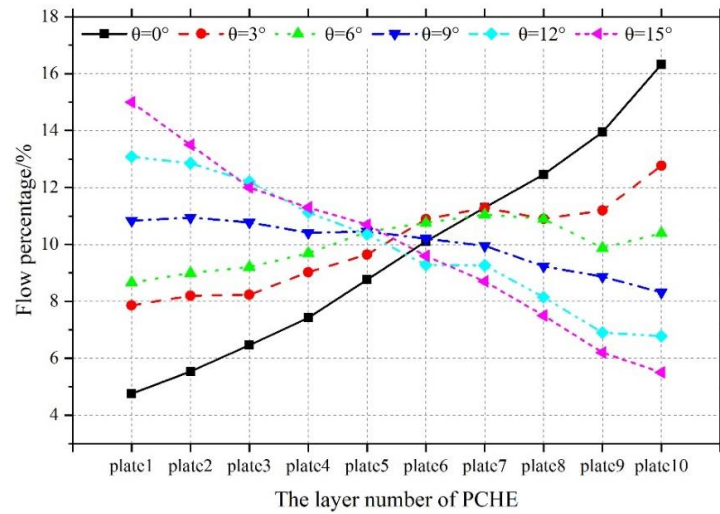


Figure 9. Flow distribution uniformity ratio of each layer.

Figure 10 shows the non-uniformity of each layer of different taper angle models, and increasing the angle of the inlet header has a significant impact on the non-uniformity of the straight barrel inlet header PCHE. As previously mentioned, $\theta = 0$ corresponds to the original configuration, and the non-uniformity of the flow rate decreases with the gradual increase in the taper angle θ when the taper angle θ is 3–12° and the number of layers is 10. This indicates that the structure of the original configuration is optimized for the taper angle, which is advantageous for uniform distribution of the flow rate in the straight barrel inlet header PCHE to each heat exchanger plate layer. With an increase in the taper angle θ , the results indicate that the optimum taper angle θ can make the flow uniformly distribute to each layer in the straight barrel inlet header PCHE. When the taper angle θ is 6° and 9°, the non-uniformity is less than 0.5, indicating that these two structural parameters of the header can significantly reduce the non-uniformity of the internal flow distribution of the straight barrel inlet header PCHE and realize uniform flow rate in each heat exchanger plate layer. When the taper angle θ is increased to 12° and 15°, compared to 6° and 9°, it is not conducive to uniform distribution in each heat exchanger plate layer of the straight barrel inlet header PCHE. The distribution results indicate that to achieve uniform distribution in each heat exchanger plate layer, the taper angle θ of the inlet header should be taken to be between 6° and 9°.

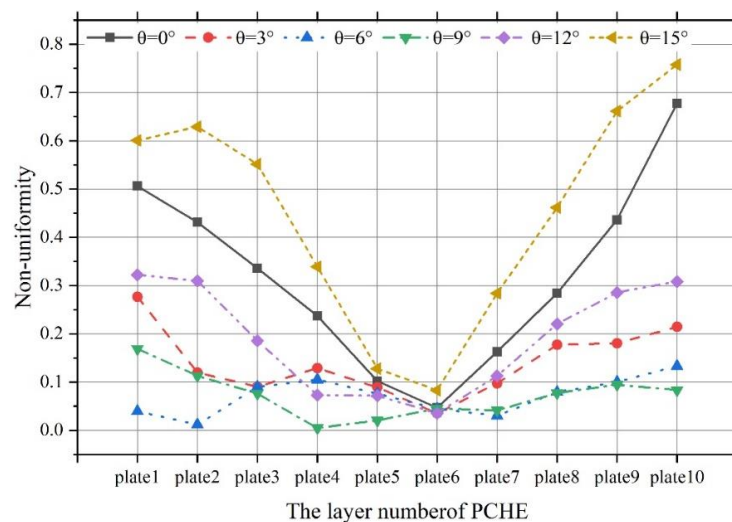


Figure 10. Non-uniformity of each layer.

For taper angles θ from 0° to 15° , Figure 11 shows the mass flow rate flow diagram and mass flow rate cloud diagram, which reflect the velocity distribution in the inlet header and each heat exchanger plate layer, and fluid streamlines showing the flow field can be observed. The existence of a backflow area can be found, and analysis of the content indicates that with increasing taper angle, the backflow dead zone decreases. When $\theta = 12^\circ$, the backflow dead zone disappears completely. The maximum local value of the mass flow rate tends to appear on the heat exchanger plate near the lower part of the header. With increasing taper angle, the red area at the entrance of the bottom heat exchanger plate gradually becomes smaller, indicating that the pointed tip of the tapered header can regulate the flow distribution ratio in each heat exchanger plate layer.

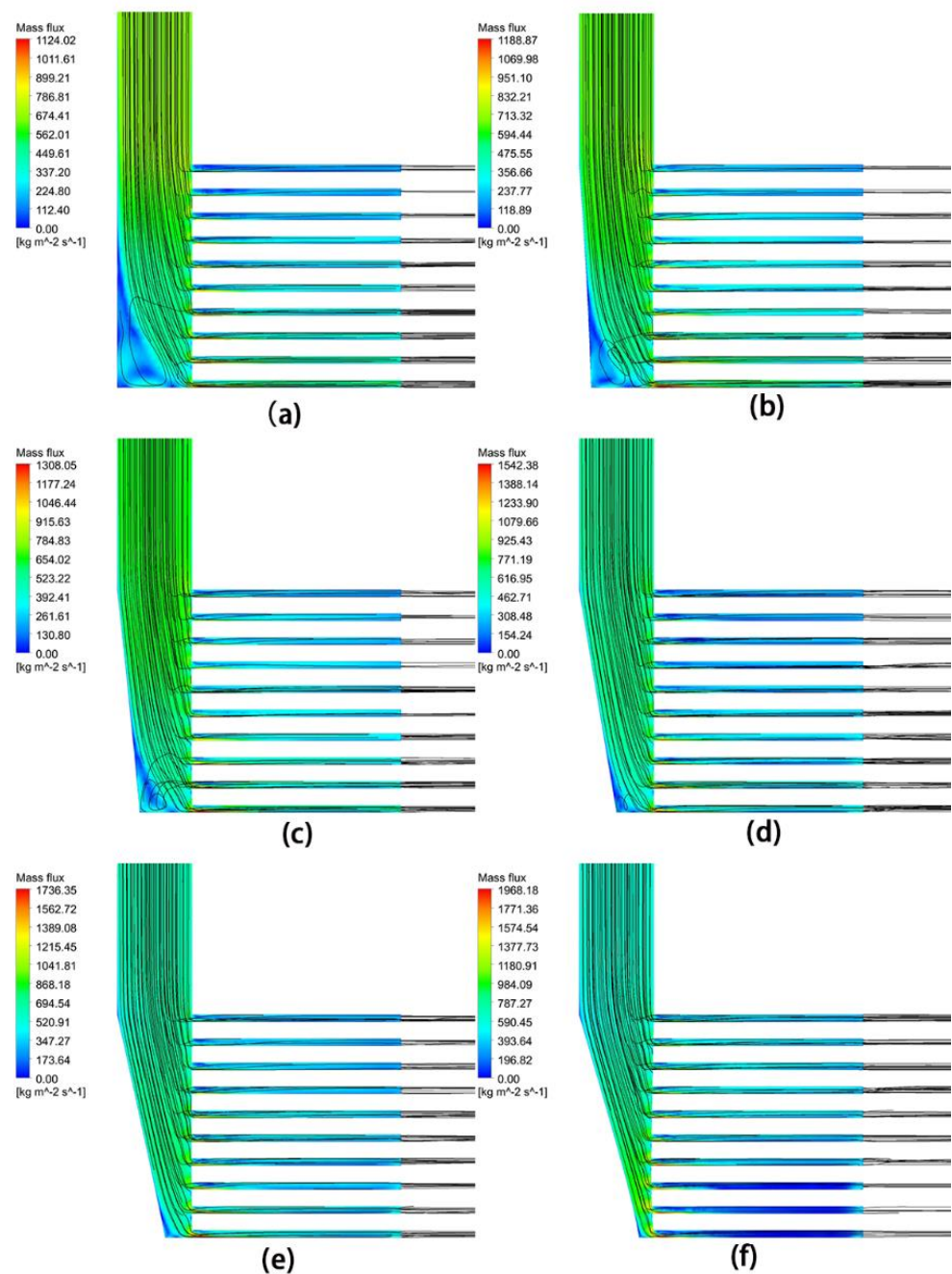


Figure 11. Mass flow rate cloud diagram and flow diagram of the headers with different angles. (a) $\theta = 0^\circ$; (b) $\theta = 3^\circ$; (c) $\theta = 6^\circ$; (d) $\theta = 9^\circ$; (e) $\theta = 12^\circ$; (f) $\theta = 15^\circ$.

Figure 12 shows the statistical results of the standard deviation (σ_p) of the non-uniformity of each layer. According to the analysis of the trend in the figure of σ_p , when the taper angle θ is 3–15°, σ_p is less than that when the taper angle θ is 0°, which indicates that optimization of the original configuration of the inlet header into a tapered header is conducive to evenly distributing the flow in the straight barrel inlet header PCHE to each heat exchanger plate layer. σ_p first decreases and then increases with decreasing angle θ , indicating an optimal taper angle θ for evenly distributing the flow in the straight barrel inlet header PCHE among all the layers. When the taper angle θ is 6° and 9°, σ_p is less than 0.05, indicating that the header with these two structural parameters can significantly reduce the non-uniformity of the flow distribution in the straight barrel inlet header PCHE and realize uniform flow distribution in each heat exchanger plate layer. When the taper angle θ increases to 12° and 15°, σ_p is greater than the corresponding value when the taper angle is 6° and 9°, which is not conducive to uniform distribution of the flow rate in each heat exchanger plate layer in the straight barrel inlet header PCHE. The distribution results show that to realize uniform flow distribution in each heat exchanger plate layer, the inlet header taper angle θ should be between 6° and 9°.

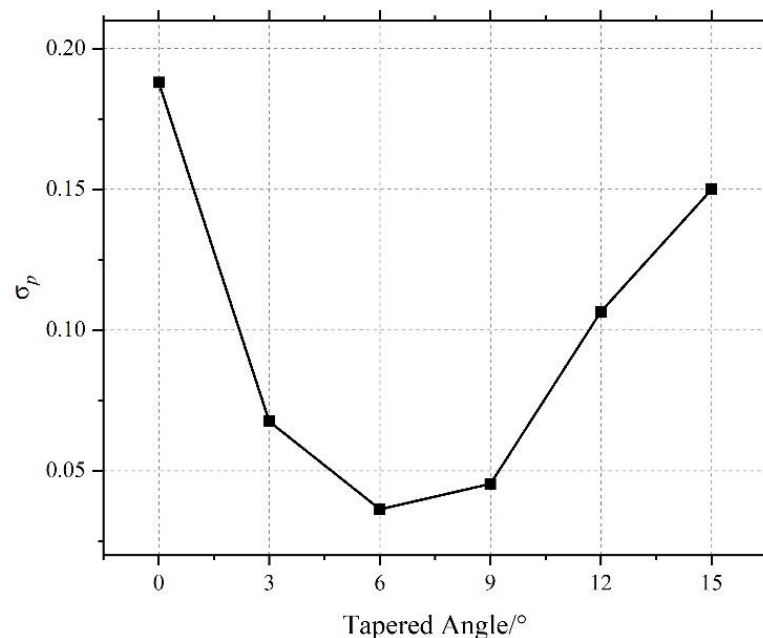


Figure 12. Standard deviation of the non-uniformity of each layer.

4. Influence of Non-Uniformity on Thermal Hydraulic Characteristics

4.1. Thermal Hydraulic Characteristics of Tapered Header PCHE

Improvement in the uniformity of the flow distribution in the PCHE strengthens the thermal hydraulic performance of the PCHE. Figure 13 shows the Nusselt numbers of models with different taper angles. Nu first increases and then decreases with increasing taper angle; that is, there is an optimal taper angle, and the Nu corresponding to this taper angle is the largest. Under the same Reynolds number, Nu is the smallest when the angle θ is 0. When the taper angle θ is 6°, Nu is the largest. When the Reynolds number is low, there is little difference in the heat transfer performance of several structures, and the difference becomes more significant with increasing Reynolds number. Comparing the optimized type with the 6° taper angle and the original type corresponding to $\theta = 0$, Nu increases by 21.3%. From the Nusselt number increasing trend, if the Reynolds number continues to grow, then the growth rate of the Nusselt number will gradually decrease; that is, the effect of increasing inlet flow rate and pressure on the PCHE will be increasingly limited.

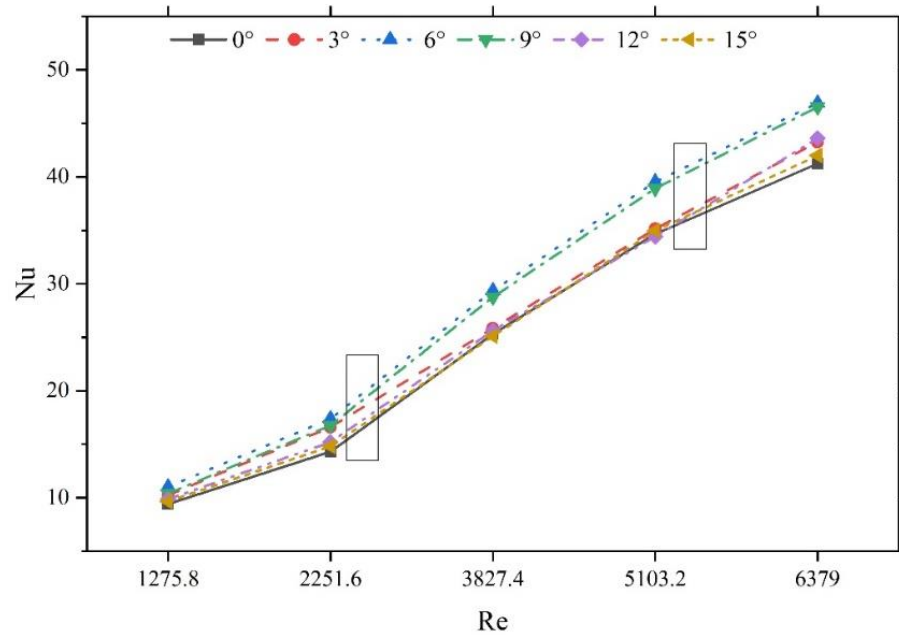


Figure 13. Nusselt numbers of different taper angle models.

Figure 14 shows the pressure drops for different taper angle models, and the pressure drop can be found to monotonically increase with increasing taper angle. The pressure drops in the five tapered models are more significant than that in the original structure; with augmentation of the heat transfer performance, the total pressure drop increases. The main reason is that the modified perturbation is more significant. The results show that the rise in the pressure drop is more strongly related to changes in the inlet header flow; the pressure drop increases by 1.6% on average with each 3° increase in the taper angle.

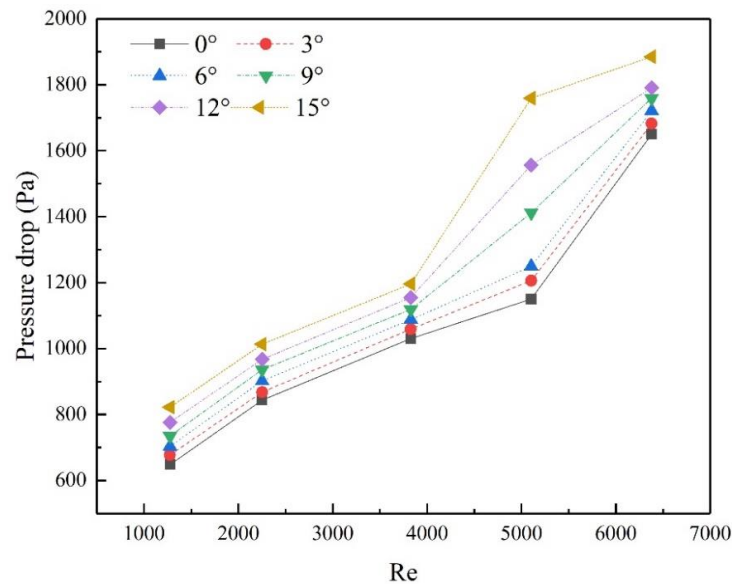


Figure 14. Pressure drops of different taper angle models.

To evaluate the comprehensive performance (*CP*) of models with different taper angles, $\frac{Nu/Nu_{ref}}{(f/f_{ref})^{1/3}}$ is adopted as the evaluation standard, where the subscript term *ref* denotes the working condition with a taper angle of 0°. Figure 15 shows the *CP* value change curves presenting the comprehensive heat transfer performance of the models with different taper angles. When the taper angle is 6°, the total heat transfer performance improves by 19.7%;

when the taper angle is 9° , the comprehensive heat transfer performance improves by 17.3%; and when the taper angle is 15° , the total heat transfer performance decreases to 98.7% that of the original configuration. The above data show that when the taper angle is between 6° and 9° , the standard deviation of the non-uniformity of the flow distribution in each layer in the straight barrel inlet header PCHE is less than 0.05. The flow distribution in each layer is relatively uniform, and the comprehensive heat transfer performance of the straight barrel inlet header PCHE can be improved by 17.3–19.7%.

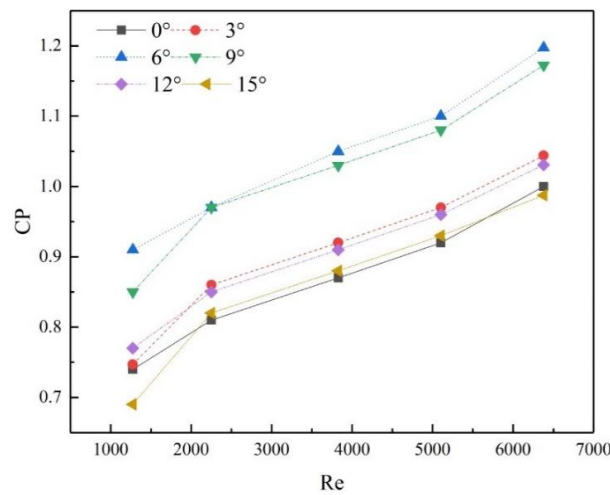


Figure 15. Comprehensive performance of models with different taper angles.

To intuitively express this relationship, the calculated results of Re, taper angle, and CP are fitted to a response surface cloud map, as shown in Figure 16. As seen from the figure, with increasing Re, CP increases. With the rise in the taper angle, CP first increases and then decreases, reaching the highest value between 6° and 9° . The red area in the figure represents the maximum CP. In this paper, reasonable matching of parameters is studied to maximize CP, reduce the non-uniformity of the flow distribution, and increase the heat exchanger performance.

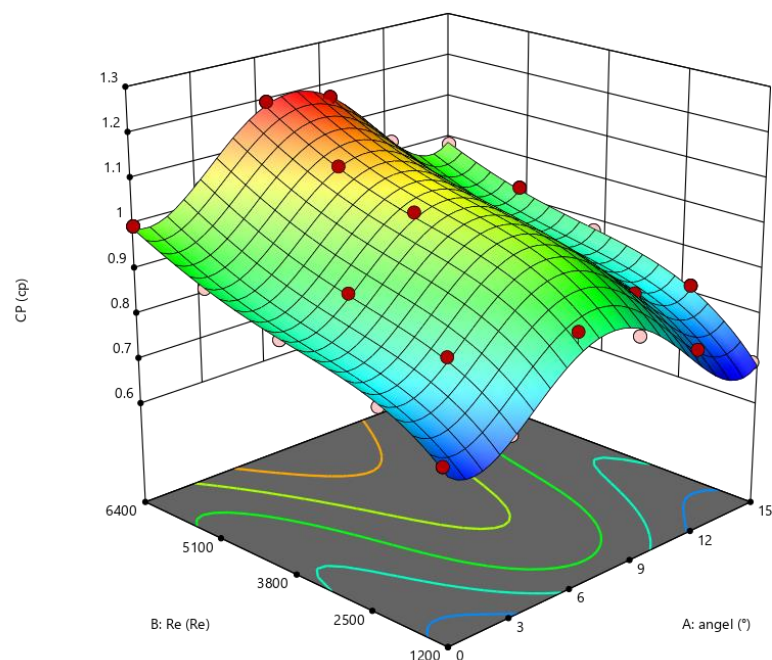


Figure 16. Relationship between design variables and target parameters.

4.2. Optimization of the Tapered Inlet Header

The genetic algorithm optimization process includes initial experimental design, response surface construction, and objective function optimization. The central combination design method is selected for experimental design, which has the characteristics of fewer tests, high precision, and good prediction. The numerical simulation results of practical design points are used to construct the response surface, approximating the relationship between the objective function and design variables. A multi objective genetic algorithm (MOGA) is used to optimize the structure based on the response surface. Optimization research based on the response surface, which is performed by using the response surface function, input, and output rather than the traditional empirical approach to avoid dealing with empirical correlations of inaccurate cases, is effective as long as its geometric model can be parameterized. The optimization goal involves quantifying the objective function, and MOGA can be used to optimize it. This section takes the PCHE as the research object and uses the two parameters of the Reynolds number and the taper angle to conduct multi parameter optimization research. The optimization ranges selected at this time are as follows: the Reynolds number range is 1000 to 6200, and the taper angle range is 0° to 15° . Based on the thermal hydraulic characteristics of the upper section, response surface methodology, and genetic algorithm, while maintaining the other parameters constant and taking CP as the objective function, the taper angle of the inlet header and the Reynolds number in operation are optimized.

4.2.1. Sensitivity Analysis

The sensitivity analysis results of the parameters can be obtained based on the response surface, and the influence degrees of the taper angle and Reynolds number on CP can be quantified. According to the sensitivity factor analysis results in Figure 17, the taper angle has the most significant influence on CP , consistent with the above analysis. The Reynolds number has a limited impact on CP . Therefore, in the design of the inlet header, the appropriate taper angle must be chosen to increase the heat transfer performance of the heat exchanger.

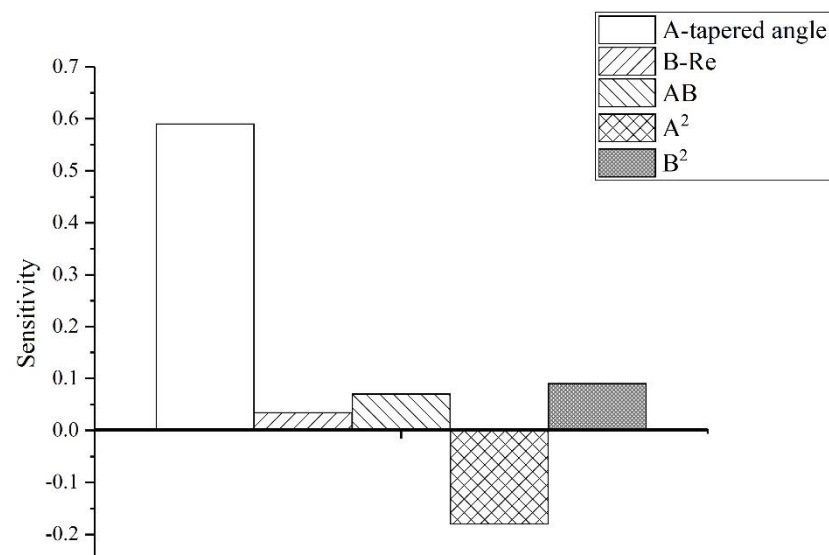


Figure 17. Sensitivity factor analysis results.

4.2.2. Optimization Results

The optimization process here mainly aims to strengthen the heat transfer (increase CP); based on the above analysis, the taper angle and Reynolds number under their joint action can produce a better heat transfer effect. The result of multi objective optimization is a series of Pareto optimal points. For the specific selection of a parameter point, for

evaluation, the actual values of the target function are considered. Figure 18 shows the degree of fitting between the model prediction(the fitting curve) and accurate simulated data(the square symbols). The model has an excellent fitting result. The variance analysis results of the response surface regression model are shown in Table 4. According to the analysis in Table 4, the F test of the total regression equation with a p -value < 0.0001 indicates very significant, and the lack of fit with a p -value > 0.05 is not significant, indicating that the whole model is meaningful and fits well. Among them, tapered angle has a significant effect on CP. The coefficient of determination of the regression model $R^2 = 0.9924$, indicating that the model can explain up to 99% of the changes, that the regression model can run in the design space, and that it is meaningful to optimize CP.

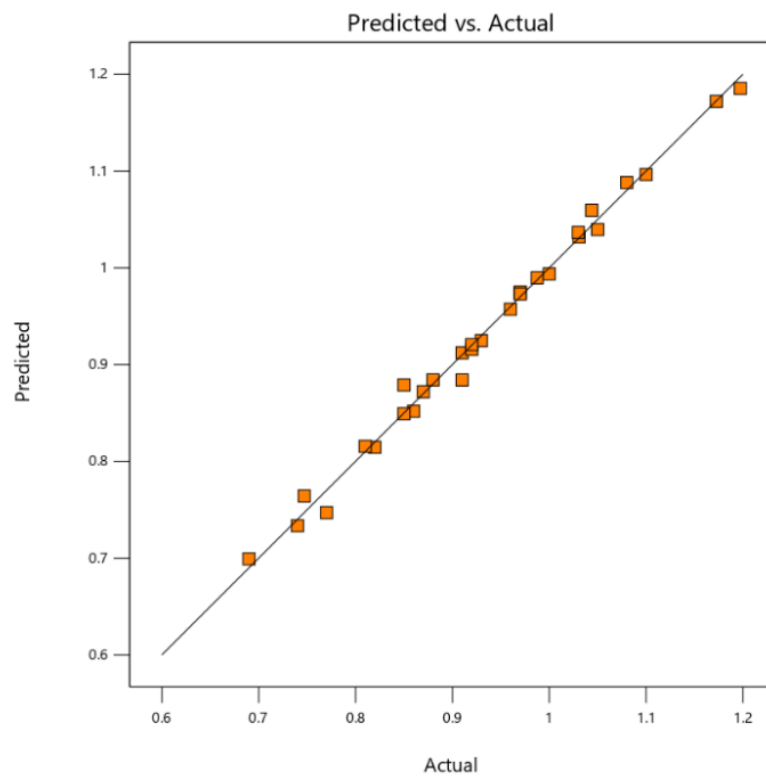


Figure 18. Comparison between model prediction and actual values.

Table 4. Variance analysis of CP regression mode.

Source	Sum of Square	Degree of Freedom	Mean Square	F-Value	p-Value	
Model	0.4431	14	0.0317	140.75	<0.0001	significant
A-Tapered Angle	0.0001	1	0.0001	0.402	0.5356	
B-Re	0.0104	1	0.0104	46.03	<0.0001	
AB	0.0002	1	0.0002	0.8928	0.3597	
A ²	0.0561	1	0.0561	249.29	<0.0001	
B ²	0.0001	1	0.0001	0.3598	0.5576	
A ² B	0.0003	1	0.0003	1.37	0.2601	
AB ²	0.0006	1	0.0006	2.58	0.129	
A ³	0.0003	1	0.0003	1.16	0.298	
B ³	0.0054	1	0.0054	23.87	0.0002	
A ² B ²	0.0002	1	0.0002	0.961	0.3425	
A ³ B	0.0002	1	0.0002	1.06	0.3193	
AB ³	0.0001	1	0.0001	0.2986	0.5928	
A ⁴	0.0322	1	0.0322	143.05	<0.0001	
B ⁴	0.0002	1	0.0002	1.04	0.3231	
Residual	0.0034	15	0.0002			
Lack of fit	0.0028	1	<0.0001	0.27	0.187	
Cor total	0.4465	29				

Taking the comprehensive heat transfer performance CP as the objective function, based on the genetic algorithm, the expected final accuracy is 10^{-3} . After 200 iterations, 10 Pareto optimal solution sets are obtained (Table 5). As seen from the table, the effect on the heat transfer performance is optimal when the taper angle is approximately 7.2° , and the Reynolds number influence on the heat transfer performance is not as strong as that of the taper angle, which is consistent with the ranges determined by numerical simulation. In addition, CP increases with increasing Reynolds number.

Table 5. Optimization results for the inlet tapered header.

Number	Angle	Re	CP	Desirability	
1	7.271	6200	1.187	0.98	Selected
2	7.209	6199.993	1.187	0.979	
3	7.152	6199.987	1.187	0.979	
4	7.456	6199.999	1.187	0.979	
5	7.047	6199.998	1.186	0.979	
6	6.938	6199.991	1.186	0.977	
7	6.374	6199.995	1.179	0.964	
8	6.228	6200.000	1.176	0.959	
9	0.000	6199.997	0.983	0.577	
10	15.000	6199.998	0.979	0.570	

5. Conclusions

In this work, we studied the flow distribution characteristics of the straight barrel inlet header PCHE by a numerical simulation method. We analyzed the flow mechanism of the extremely uneven flow distribution in each layer.

In a single flow channel, the non-uniform flow distribution phenomenon in the heat exchanger plate layers is caused by the structure itself. If a guide plate is set up in the diversion area, then a higher flow can be obtained in the middle of the channel. Nevertheless, the additional guide plate structure is bound to cause a diversion area with increased pressure drop, leading to the deterioration of the PCHE hydraulic characteristics on the whole, thus affecting the turbine inlet pressure in the Brayton cycle, which is a pyrrhic gain. In addition, due to the high operating pressure of the system, the setting of the guide plate may cause local stress concentration, which is not conducive to the safe and stable operation of the system. Therefore, the design of the existing straight barrel inlet header PCHE must be optimized to improve the non-uniformity of the flow distribution in each layer of the PCHE so that the flow in the straight barrel inlet header PCHE can be approximately evenly distributed and the system can run under conditions close to the design point.

The problem of flow matching on the cold and hot sides was analyzed according to two different layout modes of “different in and different out” and “same in and same out”. Then, the inlet header was optimized as a tapered type to find the best range of taper angles and analyze the influence of different taper angles on the thermal hydraulic characteristics of the straight barrel inlet header PCHE. The results show that when the taper angle varies from 6° to 9° , the standard deviation of the non-uniformity of the flow distribution in each layer of the straight barrel inlet header PCHE is less than 0.05, and the flow distribution in each layer is relatively uniform. The comprehensive heat transfer performance of the straight barrel inlet header PCHE can be improved by 17.3–19.7%. Finally, the response surface and a genetic algorithm were combined to optimize the inlet header. Compared with the standard structure, the heat transfer performance of the optimized system was improved by 19.7%, reaching 1.187. This study can provide theoretical guidance for the design of the PCHE inlet header.

Author Contributions: Writing—original draft preparation, K.Z.; writing—review and editing, W.W. and M.L.; software, K.Z. and Q.W.; investigation, Y.S. and M.T. All authors have read and agreed to the published version of the manuscript.

Funding: This work was supported by the High-Tech Ship Research Project of the Ministry of Industry and Information Technology (no. MIIT [2017]614) and the Fundamental Research Funds for the Central Universities (WUT: 2021IUA105).

Informed Consent Statement: Informed consent was obtained from all subjects involved in the study.

Data Availability Statement: Data are available upon reasonable request to the submitting author.

Conflicts of Interest: The authors declare no conflict of interest.

References

1. Pan, P.C.; Sun, Y.W.; Yuan, C.Q.; Yan, X.P.; Tang, X.J. Research progress on ship power systems integrated with new energy sources: A review. *Renew. Sust. Energ. Rev.* **2021**, *144*, 11048. [[CrossRef](#)]
2. Pan, P.C.; Yuan, C.Q.; Sun, Y.W.; Yan, X.P.; Lu, M.J.; Bucknall, R. Thermo-economic analysis and multi-objective optimization of S-CO₂ Brayton cycle waste heat recovery system for an ocean-going 9000 TEU container ship. *Energy Convers. Manag.* **2020**, *221*, 113077. [[CrossRef](#)]
3. Zhang, H.; Guo, J.; Huai, X.; Cui, X.; Cheng, K. Buoyancy effects on coupled heat transfer of supercritical pressure CO₂ in horizontal semicircular channels. *Int. J. Heat Mass Tran.* **2019**, *134*, 437–449. [[CrossRef](#)]
4. Zhu, B.G.; Xu, J.L.; Zhang, H.S.; Xie, J.; Li, M.J. Effect of non-uniform heating on scCO₂ heat transfer deterioration. *Appl. Therm. Eng.* **2020**, *181*, 115967. [[CrossRef](#)]
5. Liu, B.H.; Lu, M.J.; Shui, B.; Sun, Y.W.; Wei, W. Thermal-hydraulic performance analysis of printed circuit heat exchanger precooler in the Brayton cycle for supercritical CO₂ waste heat recovery. *Appl. Energy* **2022**, *305*, 117923. [[CrossRef](#)]
6. Ehsan, M.M.; Guan, Z.Q.; Klimenko, A.Y. A comprehensive review on heat transfer and pressure drop characteristics and correlations with supercritical CO₂ under heating and cooling applications. *Renew. Sust. Energ. Rev.* **2018**, *92*, 658–675. [[CrossRef](#)]
7. Pasquier, U.; Chu, W.X.; Zeng, M.; Chen, Y.T.; Wang, Q.W.; Ma, T. CFD simulation and optimization of fluid flow distribution inside printed circuit heat exchanger headers. *Numer. Heat Transf. Part A-Appl.* **2016**, *69*, 710–726. [[CrossRef](#)]
8. Koo, G.W.; Lee, S.M.; Kim, K.Y. Shape optimization of inlet part of a printed circuit heat exchanger using surrogate modeling. *Appl. Therm. Eng.* **2014**, *72*, 90–96. [[CrossRef](#)]
9. Guo, J.F.; Huai, X.L.; Cheng, K.Y.; Cui, X.Y.; Zhang, H.Y. The effects of nonuniform inlet fluid conditions on crossflow heat exchanger. *Int. J. Heat Mass Tran.* **2018**, *120*, 807–817. [[CrossRef](#)]
10. Chu, W.-x.; Ma, T.; Zeng, M.; Qu, T.; Wang, L.-b.; Wang, Q.-w. Improvements on maldistribution of a high temperature multi-channel compact heat exchanger by different inlet baffles. *Energy* **2014**, *75*, 104–115. [[CrossRef](#)]
11. Chu, W.X.; Li, X.H.; Ma, T.; Chen, Y.T.; Wang, Q.W. Study on hydraulic and thermal performance of printed circuit heat transfer surface with distributed airfoil fins. *Appl. Therm. Eng.* **2017**, *114*, 1309–1318. [[CrossRef](#)]
12. Ma, T.; Zhang, P.; Shi, H.N.; Chen, Y.T.; Wang, Q.W. Prediction of flow maldistribution in printed circuit heat exchanger. *Int. J. Heat Mass Tran.* **2020**, *152*, 14. [[CrossRef](#)]
13. Fan, J.X.; Yeom, E. Numerical investigation on thermal hydraulic performance of supercritical LNG in PCHEs with straight, zigzag, and sinusoidal channels. *J. Vis.* **2021**, *25*, 247–261. [[CrossRef](#)]
14. Shi, H.-n.; Ma, T.; Chu, W.-x.; Wang, Q.-w. Optimization of inlet part of a microchannel ceramic heat exchanger using surrogate model coupled with genetic algorithm. *Energy Convers. Manag.* **2017**, *149*, 988–996. [[CrossRef](#)]
15. Hong, X.; Duan, C.; Hao, D.; Li, W.; Yaoli, Z.; Gang, H. The optimization for the straight-channel PCHE size for supercritical CO₂ Brayton cycle. *Nucl. Eng. Technol.* **2021**, *53*, 1786–1795.
16. Lalot, S.; Florent, P.; Lang, S.; Bergles, A. Flow maldistribution in heat exchangers. *Appl. Therm. Eng.* **1999**, *19*, 847–863. [[CrossRef](#)]
17. Zhang, Z.; Mehendale, S.; Tian, J.; Li, Y. Experimental investigation of distributor configuration on flow maldistribution in plate-fin heat exchangers. *Appl. Therm. Eng.* **2015**, *85*, 111–123. [[CrossRef](#)]
18. Yang, H.Z.; Wen, J.; Gu, X.; Liu, Y.C.; Wang, S.M.; Cai, W.J.; Li, Y.Z. A mathematical model for flow maldistribution study in a parallel plate-fin heat exchanger. *Appl. Therm. Eng.* **2017**, *121*, 462–472. [[CrossRef](#)]
19. Ke, H.B.; Lin, Y.S.; Ke, Z.W.; Xiao, Q.; Wei, Z.G.; Chen, K.; Xu, H.J. Analysis Exploring the Uniformity of Flow Distribution in Multi-Channels for the Application of Printed Circuit Heat Exchangers. *Symmetry* **2020**, *12*, 314. [[CrossRef](#)]
20. Tereda, F.A.; Srihari, N.; Sunden, B.; Das, S.K. Experimental Investigation on Port-to-Channel Flow Maldistribution in Plate Heat Exchangers. *Heat Transf. Eng.* **2007**, *28*, 435–443. [[CrossRef](#)]
21. Anbumeenakshi, C.; Thansekhar, M.R. Experimental investigation of header shape and inlet configuration on flow maldistribution in microchannel. *Exp. Therm. Fluid Sci.* **2016**, *75*, 156–161. [[CrossRef](#)]
22. Redo, M.A.; Jeong, J.; Yamaguchi, S.; Saito, K.; Kim, H. Characterization and improvement of flow distribution in a vertical dual-compartment header of a microchannel heat exchanger. *Int. J. Refrig.* **2020**, *116*, 36–48. [[CrossRef](#)]
23. Zoljalali, M.; Mohsenpour, A.; Amiri, E.O. Developing MLP-ICA and MLP Algorithms for Investigating Flow Distribution and Pressure Drop Changes in Manifold Microchannels. *Arab. J. Sci. Eng.* **2022**, *47*, 6477–6488. [[CrossRef](#)]
24. Niroomand, R.; Saidi, M.H.; Hannani, S.K. A new multiscale modeling framework for investigating thermally-induced flow maldistribution in multi-stream plate-fin heat exchangers. *Int. J. Heat Mass Tran.* **2021**, *180*, 121779. [[CrossRef](#)]

25. Kim, I.H.; No, H.C. Thermal hydraulic performance analysis of a printed circuit heat exchanger using a helium-water test loop and numerical simulations. *Appl. Therm. Eng.* **2011**, *31*, 4064–4073. [[CrossRef](#)]
26. Kennedy, J.T.; Thodos, G. The transport properties of carbon dioxide. *Aiche J.* **1961**, *7*, 625–631. [[CrossRef](#)]
27. Chen, M.; Sun, X.; Christensen, R.N.; Skavdahl, I.; Utgikar, V.; Sabharwall, P. Pressure drop and heat transfer characteristics of a high-temperature printed circuit heat exchanger. *Appl. Therm. Eng.* **2016**, *108*, 1409–1417. [[CrossRef](#)]
28. Krishnakumar, K.; John, A.K.; Venkatarathnam, G. A review on transient test techniques for obtaining heat transfer design data of compact heat exchanger surfaces. *Exp. Therm. Fluid Sci.* **2011**, *35*, 738–743. [[CrossRef](#)]
29. Sama, S.; Blanco, I.; Crescente, G.; Catauro, M. A Simple Model of Heat Distribution at Various Rayleigh Number in Silicon Elastomer. In Proceedings of the 4th International Conference on Progress on Polymers and Composites Products and Manufacturing Technologies (POLCOM), Electr Network, Bucharest, Romania, 26–28 November 2020.
30. Chu, W.X.; Bennett, K.; Cheng, J.; Chen, Y.T.; Wang, Q.W. Numerical study on a novel hyperbolic inlet header in straight-channel printed circuit heat exchanger. *Appl. Therm. Eng.* **2019**, *146*, 805–814. [[CrossRef](#)]
31. Kumaran, R.M.; Kumaraguruparan, G.; Sornakumar, T. Experimental and numerical studies of header design and inlet/outlet configurations on flow mal-distribution in parallel micro-channels. *Appl. Therm. Eng.* **2013**, *58*, 205–216. [[CrossRef](#)]